1521-0103/366/2/244–250$35.00
THE JOURNAL OF PHARMACOLOGY AND EXPERIMENTAL THERAPEUTICS

https://doi.org/10.1124/jpet.118.248427
J Pharmacol Exp Ther 366:244–250, August 2018

Ocular Distribution and Pharmacodynamics of SF0166, a Topically Administered $\alpha_v\beta_3$ Integrin Antagonist, for the Treatment of Retinal Diseases[S]

Ben C. Askew, Takeru Furuya, and D. Scott Edwards

SciFluor Life Sciences, Cambridge, Massachusetts

Received February 13, 2018; accepted May 11, 2018

ABSTRACT

SF0166, a small-molecule $\alpha_v\beta_3$ antagonist, has physiochemical properties that allow distribution to the posterior segment of the eye after topical administration in an ophthalmic solution. The pharmacodynamics and ocular distribution of SF0166 were evaluated in several cell lines, chick chorioallantoic membrane assays, and models of ocular neovascularization in mice and pigmented rabbits. SF0166 inhibited cellular adhesion to vitronectin across human, rat, rabbit, and dog cell lines with IC_{50} values of 7.6 pM to 76 nM. SF0166 inhibited integrin–ligand interactions at IC_{50} values of 0.6–13 nM for human $\alpha_v\beta_3$, $\alpha_v\beta_6$, and $\alpha_v\beta_8$. SF0166 significantly decreased neovascularization in the oxygen-induced retinopathy mouse model. SF0166 distributed to the choroid and retina after topical ocular administration in amounts that substantially exceeded the cellular IC_{50} for adhesion to vitronectin; drug concentrations were maintained for >12 hours. In the laser-induced choroidal neovascularization model, topical ocular administration of SF0166 decreased lesion area compared with vehicle and was comparable to a bevacizumab injection. In the vascular endothelial growth factor–induced early neovascularization and vascular leakage model, topical ocular application of SF0166 resulted in a dose-dependent reduction in vascular leakage; the highest ocular doses tested showed comparable activity to a bevacizumab injection.

Introduction

Age-related macular degeneration (AMD) and diabetic retinopathy are leading causes of visual impairment and blindness worldwide that continue to grow in prevalence as the population ages and the incidence of diabetes mellitus increases (Congdon et al., 2004; Foster and Resnikoff, 2005; Bourne et al., 2013). Intravitreally injected inhibitors targeting vascular endothelial growth factor (VEGF) have had a significant impact on the treatment of neovascular AMD and diabetic macular edema (DME), a manifestation of diabetic retinopathy. Antagonists of $\alpha_v\beta_3$ and $\alpha_v\beta_5$ block VEGF-R2 phosphorylation and VEGF-stimulated adhesion, proliferation, and migration of endothelial cells (Terai et al., 2001; Tsou and Isik, 2001). After ocular VEGF exposure in monkeys, $\alpha_v\beta_3$ and $\alpha_v\beta_5$ are upregulated in migrating cells from pre-existing and newly formed vessels (Witmer et al., 2004). This evidence indicates a relationship between VEGF and α_v integrins and supports the investigation of α_v integrin antagonists to treat neovascular AMD and DME.

Small-molecule antagonists of $\alpha_v\beta_3$ and $\alpha_v\beta_5$ have been shown to inhibit retinal neovascularization in animal models when administered by i.p. or periocular injection (Luna et al., 1996; Wilkinson-Berka et al., 2006). JNJ-26076713, when administered orally, has been shown to inhibit retinal neovascularization in an oxygen-induced model of retinopathy of prematurity as well as inhibiting retinal vascular permeability in diabetic rats, a key early event in DME and neovascular AMD (Santulli et al., 2008).

AXT107, a 20-mer peptide that binds to $\alpha_v\beta_3$ and $\alpha_5\beta_1$, has recently been reported to suppress subretinal and retinal neovascularization in two mouse models after intraocular injection (Silva et al., 2017). In a rabbit model, injection of AXT107 significantly reduced VEGF-induced vascular leakage comparable to an injection of aflibercept, but showed a longer duration of action after a single injection.

ALG-1001 (Luminate) is reported to be a peptide inhibitor of $\alpha_v\beta_3$, $\alpha_v\beta_5$, $\alpha_5\beta_1$, and $\alpha_3\beta_1$ (Kupperman, 2015) and is being studied in clinical trials for the treatment of DME (NCT02348918) and vitreomacular adhesion (NCT02153476), by intravitreal injections.

SF0166 is a potent $\alpha_v\beta_3$ antagonist with appropriate physiochemical properties to allow distribution to the posterior segment of the eye after topical administration in an ophthalmic solution.

In this work, we describe the in vitro antiadhesion and antiangiogenic activity of SF0166, efficacy in a mouse model of

This work was supported by SciFluor Life Sciences.
https://doi.org/10.1124/jpet.118.248427.
[S] This article has supplemental material available at jpet.aspetjournals.org.

ABBREVIATIONS: AMD, age-related macular degeneration; BID, twice daily; CAM, chorioallantoic membrane; CnAOEC, canine aortic endothelial cells; CNV, choroidal neovascularization; DME, diabetic macular edema; DMSO, dimethylsulfoxide; DPBS, Dulbecco's PBS; HMVEC, human dermal microvascular endothelial cells; MS, mass spectometry; OCT, ocular coherence tomography; OIR, oxygen-induced retinopathy; PBS, phosphate-buffered saline; PDGF, platelet-derived growth factor; RAEC, rabbit aortic endothelial cells; RLMVEC, rat lung microvascular endothelial cells; VEGF, vascular endothelial growth factor.

oxygen-induced retinopathy (OIR), and in vivo ocular distribution and efficacy in Dutch-Belted rabbit models of laser-induced choroidal neovascularization (CNV) and VEGF-induced neovascularization. SF0166 is currently being investigated in two clinical trials in patients with DME (NCT02914613) and neovascular AMD (NCT02914639). Successful clinical development would provide a topically applied ocular treatment of DME and neovascular AMD that may replace intravitreal injections of anti-VEGF biologic drugs.

Materials and Methods

Test Materials and Cell Lines. SF0166-FA, (*S*)-3-(6-(difluoromethoxy) pyridin-3-yl)-3-(oxo-2-3-(3-(5,6,7,8-tetrahydro-1,8-naphthyridin-2-yl)propyl)-imidazolidin-1-yl)propanoic acid (mol. wt. of 475 g/mol), and SF0166, the 2-amino-2-methyl-2-propanol salt (mol. wt. of 565 g/mol), were manufactured by Anthem Biosciences (Bangalore, India) (Askew et al., 2014). Both forms of the test article are referred to as SF0166 in this article. The free acid form (SF0166-FA) was used in all studies except the VEGF-induced neovascularization in Dutch-Belted rabbits and the ocular distribution analyses in rabbits.

Human dermal microvascular endothelial cells (HMVEC) were from Lonza (Basel, Switzerland); rabbit aortic endothelial cells (RAEC) were from Cell Biologics (Chicago, IL); rat lung microvascular endothelial cells (RLMVEC) were from Vec Technologies (Rensselear, NY); K562 (leukemia) and HT29 (adenocarcinoma) were from American Type Culture Collection (Manassas, VA); and canine aortic endothelial cells (CnAOEC) were from Cell Applications (San Diego, CA).

Animals. This research was carried out in accordance with the *Guide for the Care and Use of Laboratory Animals* as adopted and promulgated by the National Institutes of Health and was approved by the clinical research organization's review board. Female 129SVE newborn mouse pups with mothers were obtained from Charles River Laboratories (Wilmington, MA). Male naive Dutch-Belted rabbits weighing approximately 1.5–2.0 kg were obtained from Covance (Denver, PA) or Western Oregon Rabbit (Philomath, OR). Food and water were supplied ad libitum.

Determination of Physiochemical Properties. A two-phase system plate was used for octanol/buffer partitioning to determine log D values. Octanol in equilibrium with universal buffer (0.15 M NaCl and 0.100 M each of phosphoric, boric, and acetic acids) was adjusted with NaOH to pH 2.0, 4.0, 7.4, and 9.0. SF0166 and standards in 10 mM dimethylsulfoxide (DMSO) were added to the plates for a final concentration of 10% DMSO. The plates were sealed, vortexed, and centrifuged to aid in phase settling. The assay was conducted on an ADW workstation using chemiluminescent nitrogen detection (Analiza, Cleveland, OH). Calculated log D values were corrected for background nitrogen.

To determine pKa values, SF0166 in 10 mM DMSO was diluted with 2 mM HCl and methanol to achieve final concentrations of 60% methanol, 100 μM SF0166, and 1% DMSO. The assay was conducted in 96-well plates using a pKa PRO Analyzer and Estimator software (AATI, Ames, IA). The average pH spacing between buffer points was 0.4 pH U, covering a pH range of 1.7–11.2. Four consecutive runs were conducted starting with 60% cosolvent and decreasing to 30% cosolvent buffers.

To assess permeability, SF0166 in 10 mM DMSO was diluted with 1× phosphate-buffered saline (PBS) for a final concentration of 200 μM SF0166, loaded onto a BD Gentest precoated PAMPA plate (BD Biosciences, San Jose, CA), and incubated 5 hours in the dark at ambient temperature. Samples were then diluted 20-fold with a 50:50 mixture of mobile phase components (0.1% formic acid in water:0.1% formic acid in acetonitrile) and analyzed using an Agilent Technologies (Santa Clara, CA) 1100 high-performance liquid chromatography coupled with a CTC HTC-PAL autosampler (CTC Analytics, Lake Elmo, MN) and AQUASIL C18 column (3 μM, 50 × 2.1 mm; Thermo Fisher Scientific, Waltham, MA). Time-of-flight mass spectometry (TOF MS) data were acquired using an Agilent 6538 Ultra High Accuracy TOF MS in extended dynamic range (m/z 100–1000) using generic MS conditions. Following data acquisition, exact mass extraction and peak integration were performed using MassHunter Software (Agilent Technologies).

Binding to $\alpha_v\beta_3$, $\alpha_v\beta_5$, $\alpha_v\beta_6$, and $\alpha_v\beta_8$ Integrins. SF0166 was assessed for binding to $\alpha_v\beta_3$, $\alpha_v\beta_5$, $\alpha_v\beta_6$, and $\alpha_v\beta_8$ integrins using a previously published in vitro assay (Ludbrook et al., 2003). Briefly, $\alpha_v\beta_3$, $\alpha_v\beta_5$, $\alpha_v\beta_6$, and $\alpha_v\beta_8$ integrins (R&D Systems, Minneapolis, MN) were coupled to Dynabeads M-270 Epoxy (ThermoFisher Scientific), and conditions for the binding of the coupled Dyna beads to the integrins' respective ligands were optimized. Ligands were as follows: vitronectin (R&D Systems) for $\alpha_v\beta_3$ and $\alpha_v\beta_5$; latency-associated peptide transforming growth factor-β1 (R&D Systems) for $\alpha_v\beta_6$ and $\alpha_v\beta_8$. Each integrin–ligand pair was treated with SF0166 at concentrations of 3.9–500 nM in 0.08% DMSO (triplicate measures). After a 3-hour incubation, the beads were washed, labeled with a primary antibody to the ligand (R&D Systems) and a secondary antibody conjugated with fluorescein isothiocyanate (Sigma-Aldrich, St. Louis, MO), and analyzed by flow cytometry. The method was validated by screening the effect of echistatin, cilengitide, and CWHM12 (synthesized by Anthem BioSciences) (Henderson et al., 2013) on the appropriate integrin–ligand pair. IC_{50} values were determined using Prism software (GraphPad, La Jolla, CA).

Testing of Antiadhesion Activity. The activity of SF0166 in blocking adhesion to vitronectin was assessed in HMVEC, RAEC, and RLMVEC, and in blocking adhesion to vitronectin and fibronectin was assessed in CnAOEC. (Adhesion to vitronectin is mediated by $\alpha_v\beta_3$ and $\alpha_v\beta_5$; adhesion to fibronectin is predominantly mediated by $\alpha_5\beta_1$.)

HMVEC were used at passages 9–14, and RAEC and RLMVEC cells were used at passages 4–14. Cells were grown in T175 tissue culture flasks and dislodged by gentle 3-minute treatment with Accutase. After washing, the cells in suspension in RPMI were loaded with calcein-AM (5 μM) for 30 minutes at 37°C and resuspended into RPMI without phenol red containing 10% fetal bovine serum. Assays were performed in 96-well plates, which were coated with vitronectin in PBS, pH 7.4, by incubating 50 μl 10 μg/ml solution for 1.5 hours at room temperature or overnight at 4°C. The plates were then blocked with 1% bovine serum albumin in PBS (30 minutes at room temperature) and washed with PBS. Cell suspensions were plated at a density of 5.0×10^4 (HMVEC and RAEC) or 1.0×10^5 (RLMVEC). SF0166 was added at the same time as the cells. Two lots of SF0166 were tested. The compound was tested using a maximum concentration of 1 μM with half-log dilutions. The plates were incubated for 1.5 hours at 37°C. The plates were gently washed with two cycles of aspiration of the supernatant and addition of 100 μl prewarmed fresh Dulbecco's PBS (DPBS).

CnAOEC were used at passages 4–6. Cells were grown in T75 or T175 tissue culture flasks in canine endothelial cell growth medium (Cell Applications); cells were then washed with DPBS containing 0.5 M EDTA, and then incubated 5–10 minutes with enzyme-free cell dissociation solution (Sigma-Aldrich). After washing, the cells were diluted to 400 cells/μl in canine endothelial cell growth medium. Assays were performed in 96-well plates, which were coated with vitronectin (50 μl 10 μg/ml solution; 500 ng/well) or fibronectin (1 μg/ml; 50 ng/well) in DPBS by incubating for 2 hours at room temperature. The plates were then blocked with 1% bovine serum albumin in PBS (30 minutes at room temperature) and washed with PBS. SF0166 was tested using a maximum concentration of 1 μM with half-log dilutions. After addition of SF0166, cell suspensions were added at a density of 2.0×10^4 cells/well. The plates were incubated for 1 hour at 37°C. The plates were gently washed with two cycles of aspiration of the supernatant and addition of 100 μl prewarmed fresh canine endothelial cell growth medium. An equal volume of alamarBlue (0.1 mM resazurin solution in DPBS) was added to each well and incubated for 1 hour at 37°C.

The activity of SF0166 was compared with L-000845704 (Murphy et al., 2005), a positive control, for inhibiting the binding to vitronectin

and fibronectin of HMVE, RLMVEC, K562 (leukemia), and HT29 (adenocarcinoma) cell lines. HMVEC were used at passages 9–14; RLMVEC and HT29 cells were used at passages 4–10; and K562 cells were used at passages 3–8. Cell culture and assays were conducted as described above with the following differences. Cell suspensions were plated at a density of 2.0×10^5. SF0166 was tested at 10 concentrations with a half-log dilution schedule. Cell adhesion to vitronectin was tested in duplicate or triplicate at compound concentrations ranging from 316 nM to 0.317 pM. Cell adhesion to fibronectin was tested in duplicate or triplicate at compound concentrations ranging from 200 μM to 20 nM for HMVEC and K562 cell lines and from 316 nM to 0.317 pM for HT29. The plates were gently washed with one cycle of aspiration of the supernatant and addition of 100 μl prewarmed fresh DPBS.

Fluorescence of adherent cells was measured using a multimode plate reader (Victor 2V; PerkinElmer, Waltham, MA) at excitation/emission wavelengths of 485/535 nm. IC_{50} values were calculated with Prism software by fixing the bottom of the curves to a value of blank for empty wells.

Antiangiogenic Activity Using Chick Chorioallantoic Membrane Assay—Basic Fibroblast Growth Factor–, VEGF-, and Platelet-Derived Growth Factor–Induced Models. The ovo antiangiogenic activity of SF0166 was assessed using the chorioallantoic membrane (CAM) model, a model of angiogenesis that is widely used for evaluation of antiangiogenic therapies (Ponce and Kleinman, 2003). Fertile hen eggs were procured from a hatchery and were cleaned and decontaminated with alcohol. One milliliter of albumin was removed by syringe and incubated for 8 days. CAM surfaces were grafted with gelatin sponges impregnated with 0.5–5 μg SF0166, dissolved in PBS along with 50 ng basic fibroblast growth factor, VEGF, or platelet-derived growth factor (PDGF). A total of 1 μg staurosporine was used as a positive control. The CAMs were further incubated to day 12, and on day 12 the CAMs were fixed with 4% formaldehyde in PBS, dissected, and imaged. Imaging was performed under constant illumination and magnification using a stereo microscope fitted with a digital camera. Image analysis was performed by drawing a ring around each graft and counting the number of vessels crossing the ring (blood vessel score). Data were analyzed using Excel 2007.

Ocular Distribution. The ocular uptake and ocular tissue distribution of SF0166 were assessed after a single topical ocular administration into both eyes in Dutch-Belted rabbits. The vehicle was boric acid, hydroxypropyl-β-cyclodextrin, EDTA, and benzalkonium chloride. SF0166 was administered at a concentration of 5% and a volume of 50 μl/eye (2.5 mg/eye). Plasma and the ocular tissue samples (aqueous humor, vitreous humor, sclera, and retina–choroid plexus) were collected at 1, 4, 8, and 12 hours postdose [$n = 3$ animals (six eyes) per timepoint] and stored frozen until analysis. Working solutions were prepared in 50:50 acetonitrile:water. Working solutions were combined with plasma, a 1:1 mixture of aqueous and vitreous humor, or a mixture of blank homogenized sclera, retina, and choroid to make eight-point calibration curves. Plasma samples were analyzed using a validated liquid chromatography with tandem mass spectrometry procedure. Briefly, 100 μl aliquots were mixed with 0.75 ml acetonitrile (Spectrum, New Brunswick, NJ) containing 10 ng SF0166-*d3* internal standard. After shaking for 5 minutes, the sample was centrifuged to remove precipitated proteins, and 200 μl of the resulting supernatant was transferred to an autosampler tube, diluted with 0.5 ml American Society for Testing and Materials type I water, and vortex-mixed for instrumental analysis. For the determination of SF0166 in vitreous and aqueous humor, study specimens were homogenized in a shaker for 1 hour and centrifuged, and aliquots were taken for extraction and analysis. Ocular tissue specimens were finely cut, weighed, and treated with 30 parts [extraction volume (microliter) to sample weight (milligram); three parts for lens tissue] of American Society for Testing and Materials type I water and shaken for approximately 0.5 hour. Sample extraction was repeated after the addition of 10 parts of acetonitrile (one part for lens tissue) and another 0.5 hour of shaking. The samples were then centrifuged, and aliquots were taken for extraction and analysis. The specimen aliquots (100 μl) were treated with 200 μl acetonitrile-containing internal standard and shaken for approximately 0.5 hour. The samples were then centrifuged to remove precipitated proteins and diluted with 200 μl water for instrumental analysis. Samples were analyzed using liquid chromatography with tandem mass spectrometry. Ocular pharmacokinetic parameters were determined by noncompartmental analysis using R (version 3.3.1) with the package PKNCA.

OIR Mouse Model. The efficacy of SF0166 was evaluated in the OIR mouse model. On postnatal day 7, mice were subjected to hyperoxia (75% oxygen) to inhibit retinal vessel growth and induce retinal vessel loss (vaso-obliteration). At postnatal day 12, mice were returned to a normoxic environment to induce retinal neovascularization. On postnatal days 13–17, mice received bilateral topical instillation of vehicle or 5% SF0166 twice daily (BID). At postnatal day 18, retinal tissue was collected, processed, and analyzed to measure vaso-obliteration and neovascularization.

Retinas were stained with isolectin B4 to selectively label retinal vasculature. Stained retinal flat mounts were imaged and analyzed to quantify both vaso-obliteration, defined as the avascular area central to the optic nerve, and neovascularization. Statistical analyses were performed using Prism software using an unpaired t test.

Laser-Induced CNV Model in Dutch-Belted Rabbits. In the laser-induced CNV model, the safety and efficacy of SF0166 were evaluated over 5 weeks using clinical ophthalmic exams, ocular coherence tomography (OCT), fundus photography, and fluorescein angiography. Prior to placement on study, animals underwent prescreening ophthalmic examinations, including slit-lamp biomicroscopy and indirect ophthalmoscopy. Ocular findings were scored as shown in Supplemental Table 1. Only animals with a score of 0 in all categories were included in the study. Animals were anesthetized for CNV induction, and one drop of topical proparacaine hydrochloride anesthetic (0.5%) was placed in each eye before procedures. CNV was induced by laser treatment on day −3. An external diode laser was applied to the retina using a laser contact lens and a slit-lamp biomicroscope. Both eyes of each animal underwent laser photocoagulation treatment (18–23 spots per eye sized 20–100 μm). Following laser treatment, 50 μl of a 25 μg/ml VEGF solution (1.25 μg dose) was injected intravitreally into each eye, which prolongs the viability of CNV induced by laser injury (Gum et al., 2005). Topical antibiotic ointment was applied after the laser CNV induction procedure. Overall safety was assessed through daily general health and gross ocular observations.

The test articles were SF0166, bevacizumab (Avastin) as positive control, and vehicle. The SF0166 consisted of 2.5 wt% SF0166 dissolved in PBS containing 5 wt% sulfobutyl ether β-cyclodextrin. SF0166 (1.25 mg/eye) and vehicle control were administered topically in 50 μl into each eye BID starting on day 1, except on day 35 when the terminal ocular distribution study was performed. Bevacizumab (1.25 mg/eye) was administered by intravitreal injection once on day 1.

The Heidelberg Spectralis OCT (software version 5.4) was used to capture both the OCT and fluorescein angiography images during the study. Lesion dimensions (widths and heights measured in micrometers) were measured using the OCT images and utilizing the algorithms of the Heidelberg Spectralis OCT software. Lesion sites that were more uniform in shape and away from any anomalies associated with the initial CNV induction were selected for measurements. Four sites were chosen for each eye, and the same four sites were assessed at each timepoint.

The areas of the previously measured lesions were analyzed by individually tracing the overall perimeter of the CNV anomaly using the algorithms of the Heidelberg Spectralis OCT software. Statistical analysis was performed on the area of the lesions for each eye over the course of the study, and the data were analyzed using analysis of variance. Differences among groups were analyzed using Dunnett's multiple comparison procedure.

VEGF-Induced Neovascularization Model in Dutch-Belted Rabbits. The VEGF-induced neovascularization and vascular leakage model study evaluated the safety, efficacy, and distribution of

TABLE 1
Activity of SF0166 and L-000845704 in blocking cell adhesion to vitronectin (vn) and fibronectin (fn)
N = 2–4 per group.

Compound	K562		HT29		HMVEC		RLMVEC	
	vn IC_{50}, μM	fn IC_{50}, μM	vn IC_{50}, μM	fn IC_{50}, μM	vn IC_{50}, μM	fn IC_{50}, μM	vn IC_{50}, μM	fn IC_{50}, μM
SF0166	0.00161	3.04	0.00129	0.00127	0.00105	159	0.00000761	930
L-000845704	0.00118	1.81	0.00159	0.00533	0.00110	46.3	0.0000286	239

SF0166. Prior to placement on study, each animal underwent an ophthalmic examination (slit-lamp biomicroscopy and indirect ophthalmoscopy). Ocular findings were scored as shown in Supplemental Table 2. The acceptance criteria for placement on study were scores of 0 for all variables. Neovascularization and vascular leakage were evaluated by fluorescein angiography, and the images were graded to determine the fluorescein angiography score.

Test article administration to the eyes of six Dutch-Belted rabbits per group began on day 1 of the study [2 days prior to VEGF injection (vascular leakage/neovascularization induction)]. SF0166 was dissolved in 5% hydroxypropyl β-cyclodextrin and polyethylene glycol 6000 in borate buffer. SF0166 at concentrations of 1% to 5% (0.5–2.5 mg/eye) and vehicle control were administered topically in 50 μl to each eye once daily or BID, as shown in Supplemental Table 3. Bevacizumab (1.25 mg/eye) was administered by intravitreal injection once on day 1.

Vascular leakage was induced on day 3 via intravitreal injection of VEGF (500 ng/eye). Clinical ophthalmic examinations and fluorescein imaging were performed at baseline (day −2) prior to the initiation of dosing and prior to termination on day 8. Body weights were recorded prior to the start of dosing and prior to termination. Overall safety was assessed through daily general health observations.

The fluorescein angiography images were evaluated according to the scale shown in Supplemental Table 2 to provide a mean fluorescein angiography score.

Results

Physiochemical Properties

SF0166 is an anionic molecule, marginally more lipophilic than hydrophilic, with a high membrane permeability. SF0166 has physiochemical properties as follows: log D (corrected) of −0.13 at pH 2.0; 0.62 at pH 4.0, 0.43 at pH 7.4, 0.01 at pH 9.0; pKa of 4.24 and 7.71; and permeability of 7.72×10^{-7} cm/s.

In Vitro Studies

SF0166 inhibited human integrin–ligand interactions at IC_{50} values of 0.6 nM for $\alpha_v\beta_3$, 8 nM for $\alpha_v\beta_6$, and 13 nM for $\alpha_v\beta_8$. SF0166 did not inhibit binding to $\alpha_v\beta_5$. The IC_{50} values for inhibition of cell adhesion to vitronectin were 59 nM for human (HMVEC), 76 nM for dog (CnAOEC), 49 nM for rabbit (RAEC), and 7.8 nM for rat (RLMVEC). The IC_{50} values for inhibition of cell adhesion to fibronectin were >1.0 μM for dog (CnAOEC). SF0166 and L-000845704 (positive control) were both potent inhibitors of cell adhesion to vitronectin, with IC_{50} values from 7.6 pM to 1.6 nM (SF0166) and 29 pM to 1.6 nM (L-000845704), depending on the cell line (Table 1). Both were substantially less potent in blocking cell adhesion to fibronectin, with IC_{50} values of 1.3 nM to 930 μM (SF0166) and 5.3 nM to 239 μM (L-000845704).

In the CAM assay, angiogenesis stimulated by basic fibroblast growth factor was inhibited in a dose-dependent manner, with a 36% reduction in vessel score at 0.5 μg, 42% at 1 μg, and 58% at 4 μg compared with 67% for 1 μg staurosporine, a pan-kinase inhibitor used as the positive control (Fig. 1A). Angiogenesis stimulated by VEGF was inhibited in a potent dose-dependent manner, with a 61% reduction in vessel score at 2 μg and 88% at 5 μg compared with 90% for 1 μg staurosporine (Fig. 1B). Angiogenesis stimulated by PDGF

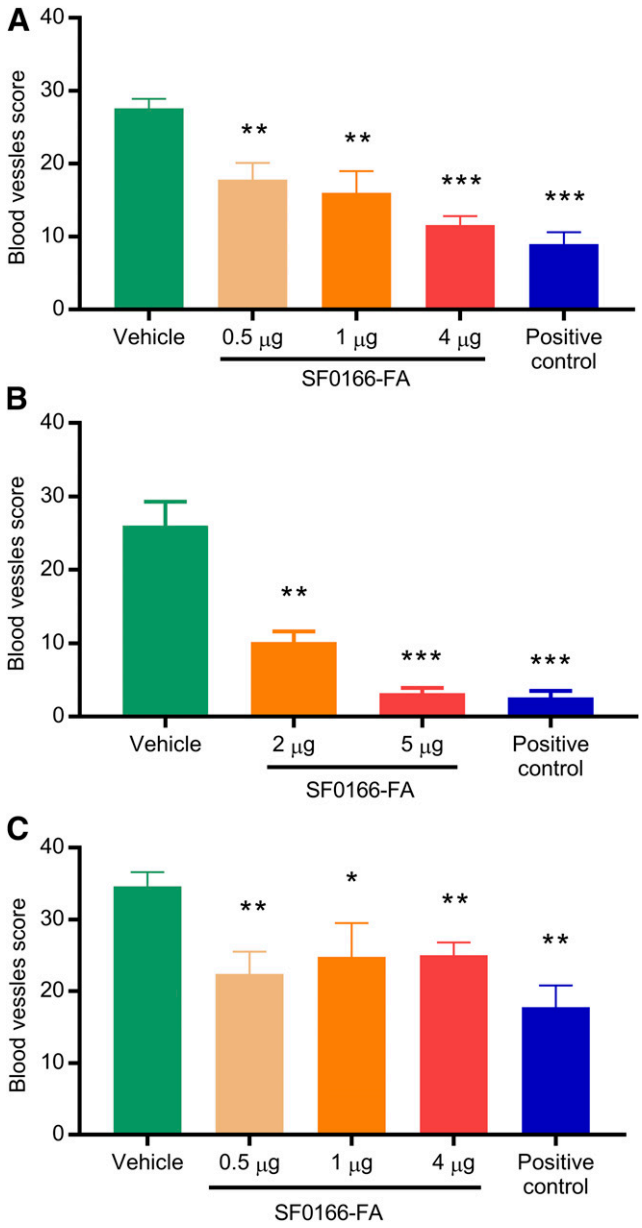

Fig. 1. Activity of SF0166 in CAM assay. (A) Basic fibroblast growth factor stimulation. (B) VEGF stimulation. (C) PDGF stimulation. Y-axis: blood vessels score. A total of 1 μg staurosporine was used as a positive control. Error bars represent S.E.M. N = 5 per group. P values for all treated groups were calculated by comparing with the vehicle group. *P < 0.05; **P < 0.01; ***P < 0.001.

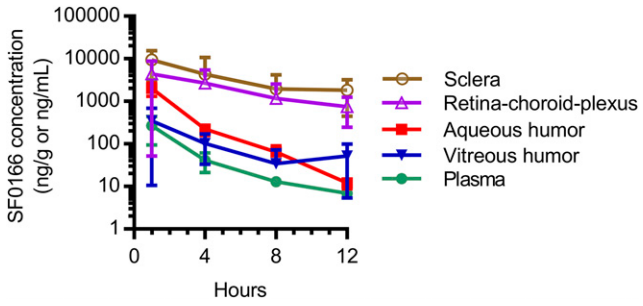

Fig. 2. Mean (error bars represent S.D.) concentrations of SF0166 in plasma, aqueous humor, vitreous humor, and ocular tissues after a single ocular administration of 5% SF0166 to Dutch-Belted rabbits. $N = 3$ animals (six eyes) per timepoint; mean of right eye and left eye combined. Units are nanograms per gram for sclera and retina–choroid plexus and nanograms per milliliter for plasma, aqueous humor, and vitreous humor.

was moderately inhibited, with a moderate 35% reduction in vessel score at 0.5 μg, 28% at 1 μg, and 28% at 4 μg with no clear dose response. Inhibition with 1 μg staurosporine was 49% (Fig. 1C).

Ocular Distribution

After a single ocular dose, rapid exposure to SF0166 was evident in all rabbits, as indicated by plasma, sclera, retina–choroid, vitreous humor, and aqueous humor C_{max} values at 1 hour postdose (the first sampling timepoint) for most tissues (Fig. 2). Ocular tissue pharmacokinetic parameters are shown in Table 2. The concentration of SF0166 in the retina–choroid peaks at 5103 ng/g or 9.0 nmol/g (formula weight of SF0166 is 565 g/mol), or ~9 μM (assuming a tissue density of 1 g/ml).

OIR Model

An increase in vaso-obliteration was seen in the group of mice treated with 5% SF0166 relative to the vehicle-treated group, but the difference was not significant ($P = 0.1412$). A significant decrease in neovascularization was observed in the 5% SF0166 treatment group relative to the vehicle treatment group (Fig. 3; $P = 0.0363$).

Laser-Induced CNV Model

There were no notable abnormalities in daily general health and gross ocular observations.

Clinical Ophthalmic Examinations. On day 0, 3 days after laser treatment and the day before initiation of dosing with SF0166, vehicle, or bevacizumab, animals across groups had scores of 1 or 2 for choroidal/retinal inflammation, retinal hemorrhage, retinal detachments, and vitreal hemorrhage.

Animals treated with SF0166 did not demonstrate any sign of ophthalmic toxicity that was not also present at the same or higher frequency in animals treated with bevacizumab or vehicle. On day 35 (treatment with SF0166 or vehicle for 34 days), all scores were 0–1 on all measures except lens (score of 3 for all animals except one animal in the SF0166 group). Scores of 1 were reported in all groups for cornea and surface area of cornea involvement, retinal detachments, and retinal hemorrhage. Small particles were still present on the posterior capsule of the lens for most animals in all dose groups.

CNV Lesion Area Measurements. Lesion area in the right eye decreased significantly in the SF0166 group compared with the vehicle control group from day 4 to the end of the study, and in the bevacizumab group from day 18 to the end of the study (Fig. 4A). [Comparison between the SF0166 and bevacizumab groups was not attempted since the starting (day 0) lesion areas were greater for the bevacizumab group (left eye and right eye).] The SF0166 group showed the most decrease in CNV lesion area in the left eye, decreasing significantly compared with the vehicle control group from day 18 to the end of the study (Fig. 4B).

VEGF-Induced Neovascularization Model

There were no notable abnormalities in daily general health observations.

Clinical Ophthalmic Examinations. Observations at the clinical ophthalmic examination on day 8 such as slight opacity of the posterior capsule or lens or of the vitreous humor, small localized retinal detachment, and cataract were all mild and may have been artifacts from intravitreal injections or immune reactions to the VEGF administration.

Fluorescein Imaging. Fluorescein image scoring indicated that the VEGF-induced vascular leakage (vehicle control group) was noticeably attenuated both in the bevacizumab group and in all SF0166-treated groups (Fig. 5). The highest degree of leakage occurred in the vehicle group. There was a dose-dependent decrease in the mean fluorescein angiography scores (attenuation of leakage) for SF0166-treated groups. The lowest mean fluorescein angiography score was in the bevacizumab group; however, the highest SF0166 dose groups showed comparable mean scores to bevacizumab. Representative fluorescein images are provided in Supplemental Fig. 1.

Discussion

This is the first report of the preclinical pharmacologic activity of an $\alpha_v\beta_3$ inhibitor administered in an eye-drop formulation. Previous studies of $\alpha_v\beta_3$ inhibitors in retinal disease models have used intraocular or i.p. injection, or oral

TABLE 2

Ocular pharmacokinetic parameters after a single ocular administration of 5% SF0166 (2.5 mg/eye) to Dutch-Belted rabbits

Values are mean (S.D.), except for T_{max} and T_{last}, which are median (range). Values are mean of right eye and left eye combined. $N = 12$ animals (six eyes per timepoint). Units are nanograms per milliliter for aqueous and vitreous humors and nanograms per gram for sclera and retina–choroid plexus.

Sample	C_{max} (ng/ml or ng/g)	T_{max} (h)	C_{last} (ng/ml or ng/g)	T_{last} (h)	$AUC_{0\text{-}last}$ (h×ng/ml or h×ng/g)
Aqueous humor	2033 (720)	1 (1, 1)	12.0 (3.19)	12 (12, 12)	5126 (1550)
Vitreous humor	352 (334)	1 (1, 4)	52.3 (47.0)	12 (12, 12)	1298 (986)
Sclera	9417 (6156)	1 (1, 1)	1845 (1394)	12 (12, 12)	45,699 (33,078)
Retina–choroid plexus	5103 (4368)	1 (1, 8)	751 (506)	12 (12, 12)	24,395 (17,534)

AUC, area under the curve.

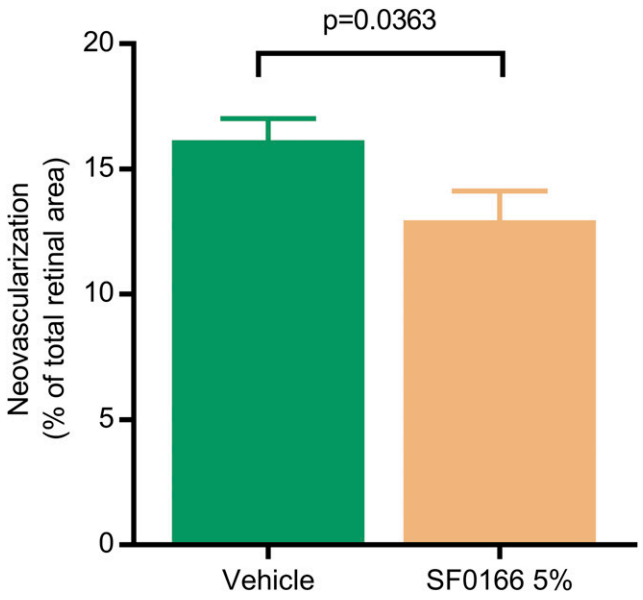

Fig. 3. Mean (error bars represent S.E.M.) neovascularization in the OIR mouse model. Mice were subjected to hyperoxia postnatal days 7–12. On postnatal days 13–17, mice received vehicle or 5% SF0166 BID. Retinal tissue was collected on postnatal day 18. $N = 7$ animals (14 eyes) per group; right eye and left eye scores combined. Statistical analysis based on unpaired t test.

dosing. These studies provide validation of inhibiting $\alpha_v\beta_3$ for the treatment of retinal disease such as neovascular AMD and DME. The only $\alpha_v\beta_3$ inhibitor that has been tested in patients is ALG-1001, which must be delivered by intravitreal injection. A topically applied $\alpha_v\beta_3$ inhibitor would potentially eliminate the need for repeated intravitreal injections.

SF0166 is the result of a drug discovery effort to synthesize small-molecule $\alpha_v\beta_3$ antagonists having the appropriate physiochemical properties to allow distribution to the posterior segment of the eye after topical administration in an ophthalmic solution. A series of analogs of L-000845704, the small-molecule $\alpha_v\beta_3$ antagonist clinically tested as a treatment of osteoporosis (Murphy et al., 2005), with a range of physiochemical properties (e.g., LogP), were synthesized by incorporating one or more fluorine substituents, testing their potency as inhibitors of cellular adhesion to vitronectin, and then advancing the compounds with potency comparable to L-000845704 into in vivo testing of ocular distribution and in models of retinal neovascularization and vascular leakage.

SF0166 inhibits ligand binding to the integrins $\alpha_v\beta_3$, $\alpha_v\beta_6$, and $\alpha_v\beta_8$ with nanomolar activity, but does not inhibit binding to $\alpha_v\beta_5$ or cellular binding to fibronectin via $\alpha_5\beta_1$. This integrin selectivity differs from that reported for the other $\alpha_v\beta_3$ antagonists tested as potential treatments for retinal diseases. ALG-1001 is reported to inhibit $\alpha_v\beta_3$, $\alpha_v\beta_5$, $\alpha_5\beta_1$, and $\alpha_3\beta_1$ (Kupperman, 2015), whereas SB-267268 and JNJ-26076713 inhibit $\alpha_v\beta_3$ and $\alpha_v\beta_5$ (Wilkinson-Berka et al., 2006; Santulli et al., 2008), and AXT107 inhibits $\alpha_v\beta_3$ and $\alpha_5\beta_1$ (Silva et al., 2017). Despite the absence of activity against $\alpha_v\beta_5$ and $\alpha_5\beta_1$, SF0166 was effective in models of retinal neovascularization and vascular leakage. The potential implications of the inhibitory activity of SF0166 against $\alpha_v\beta_6$ and $\alpha_v\beta_8$ receptors remain to be determined.

SF0166 distributed to the choroid and retina after topical ocular administration in amounts that substantially exceeded the IC_{50} value for binding to $\alpha_v\beta_3$ and for cellular adhesion to vitronectin, and these high drug concentrations were maintained for more than 12 hours. The high levels of SF0166 in the sclera and low levels in the vitreous show a scleral route of distribution to the back of the eye. In the laser-induced CNV model in pigmented rabbits, topical ocular administration of SF0166 decreased lesion area compared with vehicle and was comparable to an injection of bevacizumab. In the VEGF-induced rabbit early

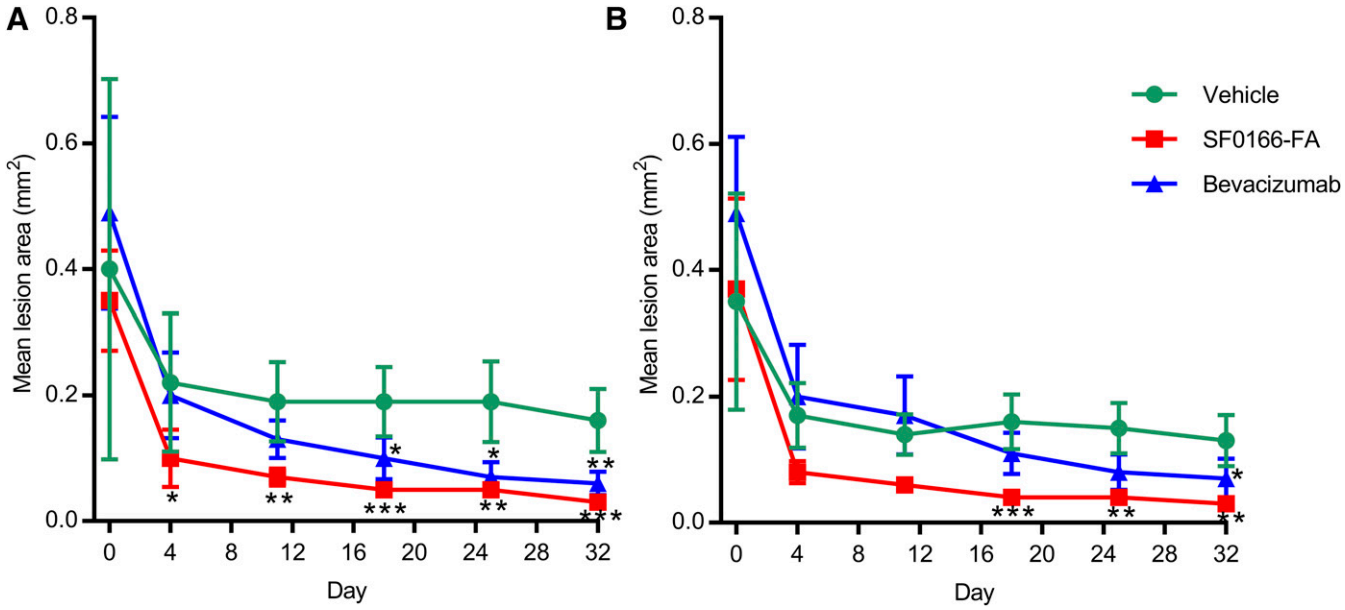

Fig. 4. Mean (error bars represent S.D.) CNV lesion area at specified timepoints (study days). (A) Right eye. (B) Left eye. CNV was induced by laser treatment on day −3. Lesion area measurements were performed on day 0; dosing started on day 1 (2.5% BID SF0166; single injection of 1.25 mg/eye bevacizumab). $N = 24$ lesions per group (four lesions per eye, three animals per group). Postdose lesion area measurements were made weekly starting on day 4. Statistical analysis based on analysis of variance with Dunnett's multiple comparison test: $^*P < 0.05$; $^{**}P < 0.01$; $^{***}P < 0.001$ (all comparisons to vehicle group). The same lesions (four/eye) were tracked throughout study.

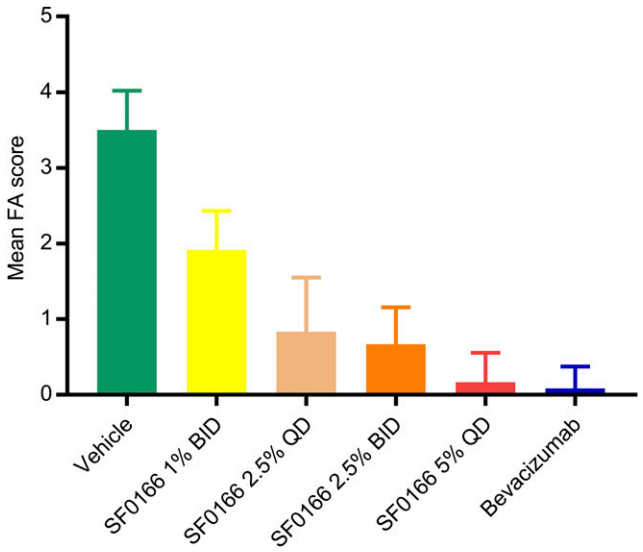

Fig. 5. Mean (error bars represent S.D.) vascular leakage measured by fluorescein angiography. Vascular leakage was induced on day 3 via intravitreal injection of VEGF (2 days after the start of study drug dosing on day 1). Fluorescein imaging was performed after 8 days of dosing (day 8) with the indicated concentrations of SF0166. $N = 6$ animals (12 eyes) per group; right eye and left eye scores combined.

neovascularization and vascular leakage model, topical ocular application of SF0166 resulted in a dose-dependent reduction in vascular leakage; the highest ocular doses tested showed comparable activity to an injection of bevacizumab. If comparable ocular concentrations can be achieved in humans after topical ocular administration, the concentration of SF0166 would be approximately 13,000-fold higher than the IC_{50} for inhibiting binding to $\alpha_v\beta_3$ and approximately 130-fold higher than the IC_{50} of SF0166 in the functional adhesion assay. If retention in retina and choroid in humans is comparable to that seen in rabbits (C_{last} = 751 ng/g at 12 hours), the SF0166 concentration would be >20-fold the IC_{50} in the functional assay. Therefore, after administering an eye drop containing 2.5 mg SF0166, $\alpha_v\beta_3$ should be nearly completely inhibited for up to 12 hours.

SF0166 topical ophthalmic solution is intended to address limitations in current treatment of neovascular AMD and DME, which include agents requiring intravitreal injection every 4–12 weeks under local anesthesia. The activity of SF0166 in VEGF-driven models appears similar to that of anti-VEGF biologic drugs (e.g., bevacizumab). Moreover, SF0166 also blocks angiogenic signaling driven by other growth factors [fibroblast growth factor and PDGF (partially)], so clinical efficacy could exceed that of marketed drugs that only target VEGF.

SF0166 was efficacious in preclinical models of ocular neovascularization and vascular leakage and has completed nonclinical development, including safety pharmacology and toxicology studies required prior to testing in the clinic. SF0166 is currently being investigated in two clinical trials in patients with DME (NCT02914613) and neovascular AMD (NCT02914639). Both studies are Phase I/II, randomized, double-masked, multicenter clinical trials designed to evaluate the safety and exploratory efficacy after 28 days of SF0166 topical ophthalmic solution BID and 28 days of post-treatment follow-up.

Acknowledgments

Becky Norquist assisted with the preparation of this manuscript.

Authorship Contributions

Participated in research design: Askew, Furuya, Edwards.
Conducted experiments: Askew.
Performed data analysis: Askew.
Wrote or contributed to the writing of the manuscript: Edwards.

References

Askew BC, Heidebrecht RW, Furuya T, and Duggan ME (2014) inventors, SciFluor Life Sciences, assignee. Fluorinated 3-(2-oxo-3-(3-arylpropyl)imidazolidin-1-yl)-3-arylpropanoic acid derivatives. U.S. patent US20140221410A1; 07 August 2014.
Bourne RR, Stevens GA, White RA, Smith JL, Flaxman SR, Price H, Jonas JB, Keeffe J, Leasher J, Naidoo K, et al.; Vision Loss Expert Group (2013) Causes of vision loss worldwide, 1990-2010: a systematic analysis. *Lancet Glob Health* **1**:e339–e349.
Congdon N, O'Colmain B, Klaver CC, Klein R, Muñoz B, Friedman DS, Kempen J, Taylor HR, and Mitchell P; Eye Diseases Prevalence Research Group (2004) Causes and prevalence of visual impairment among adults in the United States. *Arch Ophthalmol* **122**:477–485.
Foster A and Resnikoff S (2005) The impact of vision 2020 on global blindness. *Eye (Lond)* **19**:1133–1135.
Gum GG, Wong CG, and de Carvalho RP (2005) Laser-induced models of choroidal neovascularization in rabbits associated with sustained suprachoroidal and episcleral delivery of VEGF and bFGF. *Invest Ophthalmol Vis Sci* **46**:1422.
Henderson NC, Arnold TD, Katamura Y, Giacomini MM, Rodriguez JD, McCarty JH, Pellicoro A, Raschperger E, Betsholtz C, Ruminski PG, et al. (2013) Targeting of αv integrin identifies a core molecular pathway that regulates fibrosis in several organs. *Nat Med* **19**:1617–1624.
Kupperman BD (2015) A dual-mechanism drug for vitreoretinal diseases. *Retina Today* July/August 2015:85–87.
Ludbrook SB, Barry ST, Delves CJ, and Horgan CM (2003) The integrin alphavbeta3 is a receptor for the latency-associated peptides of transforming growth factors beta1 and beta3. *Biochem J* **369**:311–318.
Luna J, Tobe T, Mousa SA, Reilly TM, and Campochiaro PA (1996) Antagonists of integrin alpha v beta 3 inhibit retinal neovascularization in a murine model. *Lab Invest* **75**:563–573.
Murphy MG, Cerchio K, Stoch SA, Gottesdiener K, Wu M, and Recker R; L-000845704 Study Group (2005) Effect of L-000845704, an alphaVbeta3 integrin antagonist, on markers of bone turnover and bone mineral density in postmenopausal osteoporotic women. *J Clin Endocrinol Metab* **90**:2022–2028.
Ponce ML and Kleinman HK (2003) Identification of redundant angiogenic sites in laminin alpha1 and gamma1 chains. *Exp Cell Res* **285**:189–195.
Santulli RJ, Kinney WA, Ghosh S, Decorte BL, Liu L, Tuman RW, Zhou Z, Huebert N, Bursell SE, Clermont AC, et al. (2008) Studies with an orally bioavailable alpha V integrin antagonist in animal models of ocular vasculopathy: retinal neovascularization in mice and retinal vascular permeability in diabetic rats. *J Pharmacol Exp Ther* **324**:894–901.
Silva RLE, Kanan Y, Mirando AC, Kim J, Shmueli RB, Lorenc VE, Fortmann SD, Sciamanna J, Pandey NB, Green JJ, et al. (2017) Tyrosine kinase blocking collagen IV-derived peptide suppresses ocular neovascularization and vascular leakage. *Sci Transl Med* **9**:eaai8030.
Terai Y, Abe M, Miyamoto K, Koike M, Yamasaki M, Ueda M, Ueki M, and Sato Y (2001) Vascular smooth muscle cell growth-promoting factor/F-spondin inhibits angiogenesis via the blockade of integrin alphavbeta3 on vascular endothelial cells. *J Cell Physiol* **188**:394–402.
Tsou R and Isik FF (2001) Integrin activation is required for VEGF and FGF receptor protein presence on human microvascular endothelial cells. *Mol Cell Biochem* **224**:81–89.
Wilkinson-Berka JL, Jones D, Taylor G, Jaworski K, Kelly DJ, Ludbrook SB, Willette RN, Kumar S, and Gilbert RE (2006) SB-267268, a nonpeptidic antagonist of alpha(v)beta3 and alpha(v)beta5 integrins, reduces angiogenesis and VEGF expression in a mouse model of retinopathy of prematurity. *Invest Ophthalmol Vis Sci* **47**:1600–1605.
Witmer AN, van Blijswijk BC, van Noorden CJ, Vrensen GF, and Schlingemann RO (2004) In vivo angiogenic phenotype of endothelial cells and pericytes induced by vascular endothelial growth factor-A. *J Histochem Cytochem* **52**:39–52.

Address correspondence to: Dr. D. Scott Edwards, SciFluor Life Sciences, 300 Technology Square, Cambridge, MA 02139. E-mail: scott.edwards@scifluor.com